ELSEVIER

Polymer 40 (1999) 439–445

polymer

Time-resolved SAXS study of crystallization of poly(ethylene oxide)/poly(methyl methacrylate) blends

J. Baldrian[a,*], M. Horký[b], A. Sikora[a], M. Steinhart[a], P. Vlček[a], H. Amenitsch[c], S. Bernstorff[d]

[a]*Institute of Macromolecular Chemistry, Academy of Sciences of Czech Republic, Heyrovský Sq. 2, 162 06 Prague 6, Czech Republic*
[b]*Faculty of Nuclear Sciences and Physical Engineering, Czech Technical University, V Holešovcèkách 2, 180 00 Prague 8, Czech Republic*
[c]*Institute for Biophysics and X-ray Structure Research, Austrian Academy of Sciences, Steyergasse 17, 8010 Graz, Austria*
[d]*Sincrotrone Trieste, Basovizza, 34012 Trieste, Italy*

Received 28 November 1997; revised 9 March 1998; accepted 12 March 1998

Abstract

The kinetics of structure development during isothermal melt crystallization in blends containing low-molecular-weight fractions of poly(ethylene oxide) (PEO) and poly(methyl methacrylate) (PMMA) has been investigated as a function of composition. Time-resolved synchrotron small-angle X-ray scattering, static wide-angle X-ray scattering and differential scanning calorimetry has been used. It has been found that in early stages of crystallization, PEO lamellae of the transient nonintegral folding (NIF) type in a wide range of compositions were formed. Subsequent transformation of NIF lamellae into the crystals with one-folded (1F) or extended chains (EC) has occurred through isothermal thinning or thickening. The amorphous PMMA diluent has played a decisive role in structure development. With increasing PMMA content, the induction time prior to crystal formation increased and the rates of NIF, 1F and EC crystallization decreased. Furthermore the recrystallization of the NIF crystals into either 1F or EC crystals was retarded. The addition of PMMA meant that the crystals were growing slowly in a more viscous medium and the retardation effect of the amorphous diluent on the kinetics of these processes resulted in the tendency to create stable and more perfectly ordered structures.

Keywords: Poly(ethylene oxide)/poly(methyl methacrylate) blends; Time-resolved SAXS; Isothermal crystallization

1. Introduction

Preparation of blends is one of the most effective ways for developing new polymeric materials with designed properties. Since macroscopic properties of blends are strongly influenced by their microscopic structure, an important task of blend characterization is to study phase separation and microstructure changes induced by preparation.

Blends of poly(ethylene oxide) (PEO) with poly(methyl methacrylate) (PMMA) rank among the most extensively studied systems, consisting of a crystallizable and an amorphous component. Much effort has been devoted to the study of compatibility of the PEO/PMMA systems. The investigation of melting point depression [1–4], glass transition temperature changes [3,4], measurement of spherulitic growth [2,5,6] and crystallization rates [2,4,7] showed that the components are compatible in the melt and in the amorphous phase. The determination of binary interaction parameter χ [1,8–11] gave small and negative values, which indicate a weakly interacting miscible system. A single glass transition temperature (T_g) was reported in DSC measurements for blends of PEO with atactic (a-) and syndiotactic (s-) PMMA, while two T_gs were detected in a blend with isotactic (i-) PMMA [12–14]. The results indicate that the compatibility decreases in the order s- > a- > i-PMMA.

Cimmino et al. [15] have found by small-angle X-ray scattering (SAXS) and differential scanning calorimetry (DSC) that the system PEO/i-PMMA with a relatively low molecular weight of PEO (20 000) is incompatible. Some recent papers [16,17] show incompatibility of PEO with a-PMMA. No changes of crystallinity, melting temperature, T_m, and T_g were observed in mixtures of PEO (M_n~2000 and 125 000) with a-PMMA (M_n~500 000). The increase in T_g depression was observed for blends with increasing molecular weight of low-molecular-weight fractions of PEO (< 7000) and with increasing molecular weight of PMMA [18,19]. Using low-molecular-weight PEO (8500) with a-PMMA (46 800), segregation has been found at certain compositions by inverse gas chromatography studies

* Corresponding author.

0032-3861/98/$ - see front matter
PII: S0032-3861(98)00246-8

[16]. A strong influence of molecular weight on compatibility for higher molecular weights ($> 10^5$) of a-PMMA and PEO in blends was observed [20]. A few recent investigations report on a local demixing in the disordered phase of solid PEO/a-PMMA blends [21–24].

One of the important issues is the location of amorphous diluent in the supramolecular structure of solid mixtures. As shown by SAXS, the amorphous component can reside between crystalline lamellae (s-, a-PMMA), or is excluded from interlamellar amorphous regions (i-PMMA) to interfibrillar or to interspherulite regions [2,14,21,25,26]. It was found that segregation of the amorphous diluent (PMMA) strongly depends on T_g and molecular weight [27]. The high-T_g diluent resides exclusively in the interlamellar regions, whereas the low-T_g diluent is excluded at least partially from these regions. SAXS and wide-angle X-ray scattering (WAXS) measurements also showed that with increasing M_w of PMMA, the content of PMMA in the interlamellar regions decreased [28]. A comparison of SAXS and SANS measurements supports the idea that there exists an interface at the surface of PEO lamellae from which the PMMA is excluded [21,29,30]. The changes of compatibility strongly influence the structural behaviour of the system. It may be concluded that despite all research efforts, there are conflicting reports regarding the level of mixing for PEO/PMMA, in particular concerning molecular weights of components and the tacticity of PMMA.

Studies of PEO/PMMA blends have predominantly concentrated on the investigation of compatibility and structure of higher molecular weight components. We want to contribute to an understanding of blending and structure development in these systems with low-molecular-weight components, where the crystallizable component, PEO, reveals interesting structural properties which could be influenced by blending.

It has been shown [31–35] that chains of low-molecular-weight fractions ($< 10^5$) of PEO form crystalline lamellae with an integral number of folds (IF). This has been supported by quantized change in lamellar thickness under varying crystallization conditions as observed by SAXS, DSC and EM. The most stable crystals are formed at low supercoolings without any fold: extended chain crystals (EC). In the last fewyears, it has been reported, on the basis of time-resolved synchrotron SAXS measurements, DSC and TEM results, that nonintegral-folding (NIF) crystals can be formed [36–38]. These crystals grow as a transient state and later IF lamellae are formed through an isothermal thickening or thinning process. The kinetics of the transitions of NIF to IF crystals was explained by the chain sliding diffusional motion to exclude chain ends from the lamellae to their surfaces [36].

The rate of crystallization in blends is reduced by the dilution of the crystallizable component near the growth surface. In addition, the molecular weight of components and strength of their interactions can alter both the kinetics of crystallization and the thermodynamics governing the mixing. It follows from these facts that the formation of EC, IF and NIF lamellar crystals and their development during crystallization should be different from the case of a neat polymer. The purpose of this work is to contribute to an understanding of polymer crystallization in the blends and to answer the questions: how the partially miscible diluent, PMMA, affects structure development of the crystallizable component, PEO, during isothermal crystallization from the melt; whether the crystallization conditions allow incorporation of PMMA into the interlamellar regions; and, to what extent the course of crystallization depends on the composition of blends. Time-resolved SAXS using synchrotron radiation, WAXS and DSC were used for the study of these structural phenomena.

2. Experimental

2.1. Materials

Poly(ethylene oxide) used was the low-molecular-weight fraction of M_w 3000 supplied by Fluka AG. PEO was terminated by hydroxy groups.

Atactic poly(methyl methacrylate), $M_n = 1170$, $M_w/M_n = 1.26$, $T_g = 328.2$K was used. The polymer was prepared by anionic polymerization initiated with sodium *tert*-butoxide in THF [39]. The molecular weight of polymer was controlled by addition of a calculated amount of *tert*-butylalcohol butanole to the polymerization mixture acting as a chain transfer agent, which enables the chain length of the formed polymer to be altered, particularly in the range of low-molecular-weight products [40,41]. The molecular weight of the polymer and its distribution was determined by a combination of GPC and ^{1}H NMR [1].

Neat PEO (10/0) and blends of PEO (8/2, 6/4, 4/6 and 2/8) with 80, 60, 40 and 20 wt.% PMMA were prepared by dissolving in chloroform and subsequent drying at 30°C for 2 days and then in a vacuum oven at 40°C for 1 week. Approx. 40 mg of dry samples were placed in a sample holder and used for SAXS experiments. New sample was used for each experiment.

2.2. Small-angle X-ray scattering

The time-resolved SAXS measurements were performed on the Austrian SAXS beamline at synchrotron ELETTRA in Trieste, Italy. The X-ray beam was monochromatized by an asymmetric double-crystal Si(111) monochromator, and focused onto the detector by a toroidal mirror [42]. The beam size was reduced to 0.5 × 4 mm at the position of the sample. The wavelength of X-rays was $\lambda = 1.54$ Å and the sample detector distance was 1.75 m. A one-dimensional, position-sensitive Gabriel-type delay-line detector was used to collect X-ray scattering data. The 1.6-mm-thick samples in a special holder were melted at 80°C for 20 min in an oven and then quickly inserted into

Table 1
Characterization of PEO/PMMA blends

PEO/PMMA	T_m (°C)	T_g (°C)	Cr^{WAXS}
10/0	57.6	− 67.2[a]	0.86
8/2	56.6	—	0.71
6/4	55.7	—	0.48
4/6	52.4	—	0.29
2/8	51.4	17.8	—
0/10	—	55.1	—

T_m, melting temperature; T_g, glass temperature; Cr^{WAXS}, WAXS crystallinity

the sample cell placed in the path of the X-rays, maintained at the isothermal crystallization temperature of 40°C. The crystallization temperature was reached within 60 s. Measurements consisted of 256 frames, each 10 s long. The scattering data were corrected for detector efficiency (using Fe standard) and for background and then the Lorentz correction was applied. The averaged scattering intensity of the initial melt files was taken as a background. No desmearing was performed, due to the high degree of collimation. Peak maxima and peak intensities were obtained from the corrected and smoothed intensity data. Peak positions were employed to obtain long periods according to Bragg's law, $L = 2\pi/q$ ($q = (4\pi/\lambda)\sin\theta$), where λ is the X-ray wavelength and 2Θ is the scattering angle).

2.3. Wide-angle X-ray scattering

WAXS diffraction patterns were obtained using a powder diffractometer HZG/4A (Freiberger Praezisionsmechanik GmbH, Germany). Samples were melt-crystallized for 1 h in the same way as in the case of SAXS measurements and then measured at room temperature. The crystallinities were estimated using integral intensities diffracted by crystalline and amorphous phases.

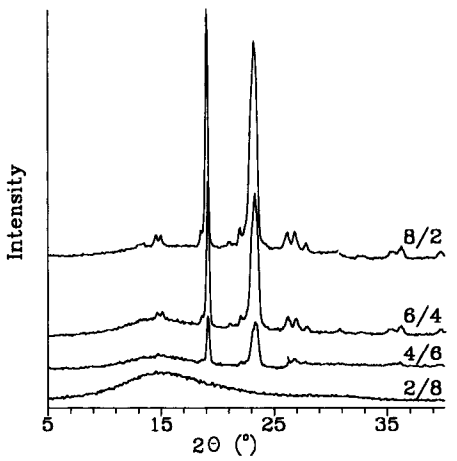

Fig. 1. WAXS patterns of PEO/PMMA blends after 1-h isothermal melt crystallization.

2.4. Differential scanning calorimetry

Differential scanning calorimetry was carried out on a Perkin Elmer DSC-2 calorimeter. The temperature and output scales of the calorimeter were calibrated using indium and sapphire as standards. The measurements were carried out in nitrogen atmosphere in the temperature interval 230–450 K. The sample weight was approx. 5 mg.

3. Results

In previously published time-resolved synchrotron SAXS measurements a blend of PEO 4000 with high-molecular-weight PMMA 170 000 was used [28]. A low-molecular-weight fraction of PEO 3000 was chosen for our experiments since it crystallizes in EC and 1F lamellar crystals and the NIF crystals are formed in a broad interval of supercooling [36–38]. We also used the low-molecular-weight fraction of PMMA 1170, as the mobility of the chains and interaction of components should be higher.

Table 1 summarizes the results of DSC measurements. The melting point decreases with increasing content of PMMA in blends. T_g of neat PMMA is near the melting points of neat PEO and PEO in blends. T_g was found only for blend 2/8 where no melting peak was observed during the cooling run. In these proportions, the components are miscible.

WAXS patterns (Fig. 1) of blends measured after 1-h isothermal melt crystallization at 40°C gave completely amorphous scattering for the 2/8 blend. Diffraction patterns of blends with higher contents of PEO show peaks corresponding to the crystalline structure of PEO. The X-ray crystallinities of blends (Table 1) decrease with increasing content of the amorphous diluent up to 60 wt.% of PMMA and then fall to zero for 80 wt.% of PMMA. From the values of WAXS crystallinity, it follows that a part of the PEO molecules was dispersed in the amorphous phase. The structure of the blends consists of crystalline PEO lamellae and an amorphous mixture, in which a part of the PEO molecules is mixed with PMMA. When the concentration of PEO is equal to or lower than 20 wt.%, the polymers are completely miscible. Similar behaviour has been reported for PEO/PMMA blends with high-molecular-weight components [3,4,10,23].

Figs 2 and 3 show Lorentz-corrected and smoothed time-resolved synchrotron SAXS data of PEO 3000 (10/0) and its 6/4 blend during isothermal crystallization at T_c = 40°C. The quality of scattering curves decreases with growing content of amorphous diluent in the blends as the content of PEO decreases and PMMA contributes to the SAXS intensity practically only by a higher level of background. Scattering peaks correspond to the fold lengths around 100, 140 and 190 Å (q~0.062, 0.045 and 0.033 Å, respectively). The fast-growing peak near 140 Å on time-resolved SAXS patterns of neat PEO and blends 8/2 and 6/4 (Fig. 2)

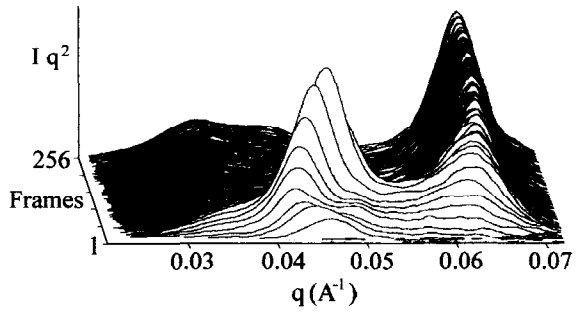

Fig. 2. Lorentz-corrected SAXS plot of crystallization of neat PEO.

corresponds to the crystallization of PEO in the NIF lamellar crystals. The NIF crystallization is not significant in the case of the 4/6 blend. In the later stages of crystallization the NIF scattering peak decreases and peaks around 100 and 190 Å gradually develop. They represent crystallization in 1F and EC crystals of PEO.

Figs 4–7 show changes in SAXS peak intensities and lamellar periodicities of PEO and blends during crystallization. For neat PEO (Fig. 4), a scattering peak with the fold length corresponding to NIF lamellae grows very quickly in the early stages of crystallization and, after reaching its maximum, decreases with a slightly slower rate. A very small part of NIF lamellae is preserved till the end of crystallization. A short time after the start of the formation of NIF lamellae, 1F and EC lamellae begin to form. A prevailing part of NIF lamellae later gradually recrystallizes into 1F lamellae. The dominant effect here is the lamellar thinning process, as it was observed before [38]. It follows from Fig. 2 that the transformation of NIF to 1F is discontinuous. No gradual change in the lamellae thickness going from NIF to 1F or EC crystals is observed. The value of the NIF periodicity starts at 127 Å and passes in early stages of crystallization through a maximum at 146 Å and a minimum at 127 Å which is followed by a very slow increase to 150 Å at the end of crystallization. Simultaneously, the fold length of 1F crystals decreases from 105 to 100 Å and this value increases from 176 to 190 Å for EC crystals.

Blend 8/2 (Fig. 5) shows similar behaviour. Again the main structure phenomenon at the beginning of the crystallization is a fast growth of NIF lamellae and later on, their recrystallization mainly to 1F and partially to EC

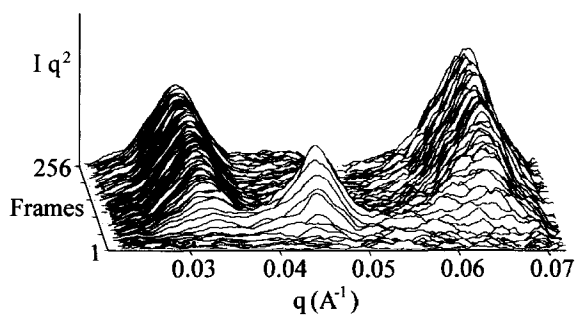

Fig. 3. Lorentz-corrected SAXS plot of crystallization of 6/4 blend.

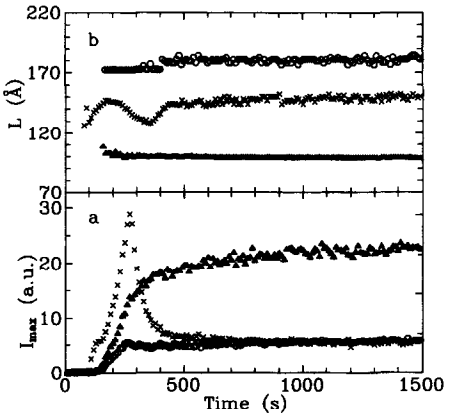

Fig. 4. Time changes of peak intensities (a) and crystal thicknesses (b) of NIF (×), 1F (▲) and EC (○) crystals during crystallization of neat PEO.

structures follows. The discontinuous lamellar thinning process also occurs here. EC and NIF lamellae are present in very small amounts at the end of crystallization. The fold length of NIF crystals starts at about 130 Å, then passes successively through a maximum at 145 Å and a minimum at 133 Å and reaches the value 148 Å at the end of the crystallization. The periodicity of the 1F structure continuously decreases from 105 to 100Å and the periodicity in the EC structure changes from 173 to 192 Å.

A higher content of PMMA in blend 6/4 causes a later start of the NIF structure formation and, with a relatively small delay, the development of 1F and EC structures (Figs 3, and 6). The amounts of 1F and EC lamellae in the 6/4 blend are practically equal during the crystallization. The isothermal thinning and thickening processes proceed simultaneously in this case. The thickness of NIF crystals starts at approx. 135 Å and then passes successively through the maximum at 140 Å and minimum at 136 Å and then slowly increases to 141 Å at the end of crystallization. The periodicity of the 1F structure decreases from 103 to 99 Å. For EC crystals this value increases from 195 to 201 Å.

The beginning of the crystalline structure formation of the

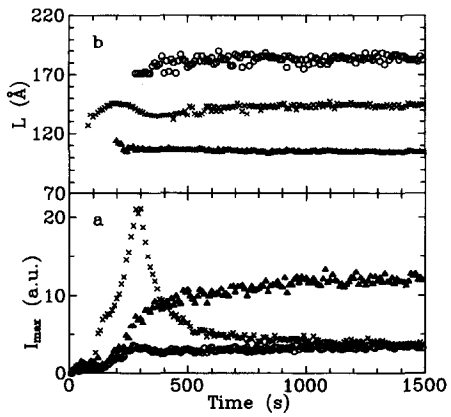

Fig. 5. Time changes of peak intensities (a) and crystal thicknesses (b) of NIF (×), 1F (▲) and EC (○) crystals during crystallization of the 8/2 PEO/PMMA blend.

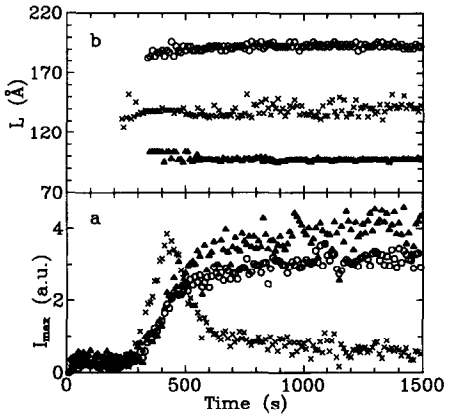

Fig. 6. Time changes of peak intensities (a) and crystal thicknesses (b) of NIF (×), 1F (▲) and EC (○) crystals during crystallization of the 6/4 PEO/PMMA blend.

4/6 blend is shifted to 1050 s for 1F crystals and to 1250 s for EC crystals after the start of crystallization. Subsequent crystallization proceeds very slowly (Fig. 7), 1F and EC structures grow simultaneously. No significant NIF crystallization is observed. From the peak intensities it follows that the content of EC lamellae is higher than that of 1F lamellae. The periodicities of both structures are 209 and 99 Å, respectively, remaining constant during the thermal treatment. Scattering curves of the 2/8 blend do not change during the thermal treatment and correspond to the one-phase amorphous structure in the melt and also in the solid state, in accordance with WAXS and DSC measurements.

In Table 2 the parameters which characterize the kinetics of structure development during crystallization of blends are summarized. In the whole series, the content of amorphous diluent PMMA strongly affects the course of the structure development during the isothermal melt crystallization. The fastest process proceeding during crystallization is the NIF structure formation. The first NIF crystals start to grow in neat PEO and the 8/2 blend after $t_c = 80$ s from the beginning of crystallization and their maximum contents are

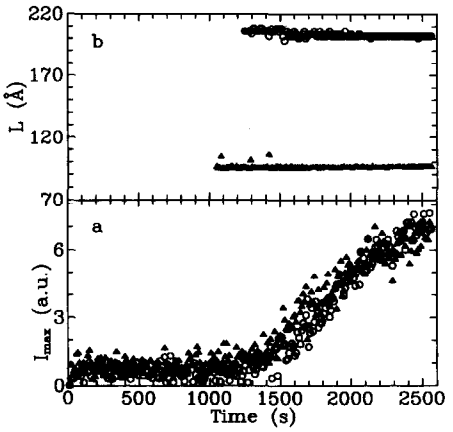

Fig. 7. Time changes of peak intensities (a) and crystal thicknesses (b) of NIF (×), 1F (▲) and EC (○) crystals during crystallization of the 4/6 PEO/PMMA blend.

reached at t_{max} 267 and 288 s, respectively. These times are much longer for the 6/2 blend, $t_c = 230$ s and $t_{max} = 430$ s. Similarly, the half-times of crystallization $t_{1/2}^{cr}$ increase from 62 s for PEO to 110 s for the 6/4 blend. With a slightly slower speed, $t_{1/2}^{rec}$, the recrystallization of the NIF structure to 1F and EC structures proceeds. In addition, this process is damped by diluting with PMMA. The recrystallization rate gradually decreases in the later stages of the process (Figs. 4(a), 5(a) and 6(a)). The formation of 1F and EC structures starts later and the rates of crystallization are much slower than in the case of NIF structures. The influence of the PMMA content on these parameters is also considerable here. The kinetics of 1F and EC structure development are similar.

4. Discussion

This is probably the first attempt to study structure changes of low-molecular-weight PEO/PMMA blends, where the constituent molecules have higher mobility. The T_g of the PMMA used is more than 50°C lower than those for common PMMA and is close to the melting points of neat PEO and PEO in the blends. Previous studies showed that the molecular weight of components is an important factor which influences structure and properties of the blends. This is why we assumed a different structural behaviour of our system. We based our study on the comparison of the results obtained for neat PEO and for PEO/PMMA blends.

DSC and WAXS measurements showed that polymers are partially miscible in a broad range of compositions. In the blends with PEO concentration higher than 30 wt.%, a two-phase system exists: crystalline PEO and an amorphous mixture of PMMA with small amounts of PEO. The 2/8 blend is amorphous with components completely miscible. A similar behaviour was obtained for previously studied PEO/PMMA blends [3,4,10,23].

The time-resolved synchrotron SAXS study demonstrates the influence of an amorphous diluent on the structure development of PEO in blends during the isothermal melt crystallization. The dominant structural phenomenon in the early stages of crystallization is the formation of NIF crystals in blends 8/2 and 6/4. This effect was previously described for low-molecular-weight fractions of neat PEO and our measurements show a similar behaviour in PEO/PMMA blends. The NIF structure is the transient state of the PEO structure. The crystals are unstable, they grow very fast and then quickly recrystallize to more stable 1F or EC structures. The NIF structure is less ordered than those into which it transforms. Two factors may contribute: chain ends incorporated in the crystals and the looseness of the fold surface structure. The formation of NIF crystals of PEO in blends is very sensitive to the amount of the second component. The growing content of the amorphous diluent increases the induction time prior to crystalline structure

Table 2
Kinetics of crystalline structure development in PEO/PMMA blends

PEO/PMMA	NIF t_c (s)	t_{max} (s)	$t_{1/2}^{cr}$ (s)	$t_{1/2}^{rec}$ (s)	1F t_c (s)	$t_{1/2}^{cr}$ (s)	EC t_c (s)	$t_{1/2}^{cr}$ (s)
10/0	80	267	62	62	160	120	170	120
8/2	80	288	70	86	200	140	280	125
6/4	230	430	86	110	350	170	340	150
4/6	—	—	—	—	1050	430	1250	400

t_c, induction time prior to crystal formation; t_{max}, time of the maximum content of NIF crystals; $t_{1/2}^{cr}$, $t_{1/2}^{rec}$, half-time of crystallization and recrystallization, respectively

formation and reduces crystallization and recrystallization rates of NIF crystals. The thinning and thickening processes are also influenced by this effect. The thinning process dominates in the neat PEO and in the 8/2 blend, while in the 6/4 blend, both these processes are similar. Crystallization in the 4/6 blend proceeded so slowly that PEO chains formed 1F and EC crystals directly.

The thickness of NIF lamellae continuously changes during the thermal treatment: its value passes through a maximum in crystallization and through a minimum in early stages of recrystallization. As recrystallization continues, the content of NIF crystals decreases to a very small value and their thickness gradually increases. These changes are the greatest in neat PEO and decrease with increasing content of PMMA. At the beginning of a very fast NIF crystallization, very distorted lamellae with highly loosened chain folds on the surfaces and, consequently, with short crystallized stems are formed. With the proceeding thermal treatment, the structure of NIF lamellae improves and their thickness slightly increases. The recrystallization starts with better developed, thicker lamellae and the mean lamellar thickness of NIF lamellae decreases. The structure of a small residue of non-recrystallized NIF lamellae continuously improves during the following phase of crystallization and the crystal thickness again increases. A lower rate of crystallization in the presence of PMMA in comparison with that for neat PEO is reflected in greater starting thicknesses of NIF lamellae and corresponds also with smaller changes of the lamellar periodicity during the thermal treatment.

SAXS experiments show that during the crystallization of PEO and its blends, besides the NIF crystals, also crystalline lamellae with thicknesses ~190 and 105 Å are formed. These periodicities represent EC lamellae with disordered surfaces, formed by chain ends only, and integrally folded 1F lamellae with disordered surfaces consisting of chain folds and ends. The PEO chains could also form double-layer lamellae from two coupled 1F chain units, the thickness of which is near to the EC crystal thickness [44] and which could hardly be distinguished from EC crystals by SAXS measurements. The formation of 1F and EC crystals in blends begins with a relatively short time lag after the start of NIF crystal formation, in the time when a significant part of the material is a supercooled melt. We suppose that first the EC and 1F structures in blends crystallize directly from the melt and that the main process—recrystallization from NIF structure—starts later. The growing content of the amorphous diluent progressively reduces crystallization rates and slowly diffusing PEO chains show a tendency to form gradually more stable structures in the order NIF, 1F, EC. For this reason, lamellar thinning was dominant in PEO and the 8/2 blend. In blend 6/4, lamellar thinning and thickening were equivalent processes. Only the direct 1F and EC crystallization occurred in the 4/6 blend and the development of EC crystals dominated.

In the early stages of crystallization, the 1F, EC and NIF lamellae are of similar quality, the widths of corresponding reflections are comparable. While the quality of the NIF crystal structure practically does not change during the thermal treatment, the 1F and EC structures continuously improve. From the widths of SAXS peaks it follows that this process also depends on the degree of dilution with PMMA. A higher dilution reduces the rate of crystallization and the PEO chains have time for the development of better ordered crystalline lamellae. The improvement of the structure during crystallization causes an increase in the EC crystal thickness of 173 to 209 Å and a small decrease in the 1F crystal thickness of 105 to 99 Å. The small change of about 6 Å for 1F crystals does not depend on the PMMA content. The maximum thickness of EC crystals occurs in the 4/6 blend and reaches the value 209 Å. This is a relatively large change in comparison with usual values for neat PEO 3000 of 195 Å.

The important question of the structure formation in PEO/PMMA blends is the location of the amorphous diluent. Recently it has been shown [28] that a low-T_g diluent is excluded at least partially from the interlamellar regions, which could be the case of our system. The first question is the location of PMMA in very rapidly growing NIF crystals. A portion of PMMA molecules from homogeneous supercooled melt could be trapped between the NIF lamellae during this very fast process. As the mean thickness of NIF lamellae decreased with increasing content of PMMA, it is not probable that the amorphous diluent was present in interlamellar regions.

The retardation effect of the amorphous diluent on 1F and EC crystallization allows enough time for the diffusion of PMMA molecules from interlamellar regions. This corresponds with final crystal thicknesses of these structures, which are comparable with the published values. An exception is the relatively high thickness of EC lamellae reached

at the end of crystallization of the 6/4 and 4/6 blends. A prerequisite for such thickening of EC crystals would be penetration of PMMA molecules between lamellae during crystallization. Another explanation of the EC thickening could be based on the assumption that the thickness of double-layer (DL) lamellae [44] is smaller than the thickness of EC lamellae. During the relatively fast crystallization of neat PEO and the 8/2 blend, DL crystals are formed and the higher content of the amorphous diluent in the 6/4 and 4/6 blends improves the crystallization conditions to such a level that more stable EC crystals are predominantly formed. No conclusive decision concerning these two possibilities can be made here.

Acknowledgements

We thank the Grant Agency of the Czech Republic and the Grant Agency of the Academy of Sciences of the Czech Republic for support with grants Nos. 103/95/0670, 203/96/1387, 106/96/1384, A4050605 and 12/96/K.

References

[1] Cortazar MM, Calahorra ME, Guzman GM. Eur Polym J 1982;18:165.
[2] Martuscelli E, Pracella M, Ping Yue W. Polymer 1984;25:1097.
[3] Li X, Hsu SL. J Polym Sci, Polym Phys Ed 1984;22:1331.
[4] Liberman SA, Gomes AS, Macki EM. J Polym Sci, Polym Chem Ed 1984;22:2809.
[5] Calahorra E, Cortazar M, Guzman GM. Polymer 1982;23:1322.
[6] Bartczak Z, Martuscelli E. Makromol Chem 1987;188:445.
[7] Calahorra E, Guzman M. Polym Commun 1983;24:211.
[8] Ito H, Russell TP, Wignall GD. Macromolecules 1987;20:2213.
[9] Hopkinson I, Kiff FT, Richards RW, King SM, Farren T. Polymer 1995;36:3523.
[10] Privalko VP, Petrenko KD, Lipatov YuS. Polymer 1990;31:1277.
[11] Pedemonte E, Polleri V, Turturro A, Cimmino S, Silvestre C, Martuscelli E. Polymer 1994;35:3278.
[12] Cimmino S, Martuscelli E, Silvestre C. Makromol Chem, Macromol Symp 1988;16:147.
[13] Zawada JA, Ylitalo CM, Fuller GG, Colby RF, Long TE. Macromolecules 1992;25:2896.
[14] Silvestre C, Cimmino S, Martuscelli E, Karasz FE, McKnight WJ. Polymer 1987;28:1190.
[15] Cimmino S, Di Pace E, Martuscelli E, Silvestre C. Makromol Chem, Rapid Commun 1988;9:261.
[16] Murakami Y. Polym. J. 1988;20:549.
[17] Privalko VP, Lipatov YuS, Petrenko KD. Polym Sci USSR (Engl Transl) 1987;29:2259.
[18] Takagashi M, Hasegawa J, Matsuda H. Rep Prog Polym Phys Jpn 1992;35:205.
[19] Takagashi M, Shimono S, Matsuda H. Rep Prog Polym Phys Jpn 1993;36:159.
[20] Marco C, Fatou JG, Gomez MA, Tanaka H, Tonelli AE. Macromolecules 1990;23:2183.
[21] Russell TP, Ito H, Wignall GD. Macromolecules 1988;21:1703.
[22] Schantz S. Polym Mater Sci Eng 1994;71:209.
[23] Straka J, Schmidt P, Dybal J, Schneider B, Spevacek J. Polymer 1995;36:1147.
[24] Schantz S. Macromolecules 1997;30:1419.
[25] Cimmino S, Di Pace E, Martuscelli E, Silvestre C. Makromol Chem 1990;191:2447.
[26] Takagashi M, Umezaki K, Yoshida H, Matsuda H. Rep Prog Polym Phys Jpn 1992;35:209.
[27] Martuscelli E, Canetti M, Vicini L, Seves A. Polymer 1982;23:331.
[28] Talibuddin S, Wu L, Runt J, Lin JS. Macromolecules 1996;29:7527.
[29] Runt JP, Barron CA, Zhang XF, Kumar SK. Macromolecules 1991;24:3466.
[30] Barron CA, Kumar SK, Runt JP, Fitzgerald J. Polym Mater Sci Eng 1991;65:333.
[31] Kovacs AJ, Gonthier A. Kolloid Z Z Polym 1972;250:530.
[32] Kovacs AJ, Gonthier A, Straupe C. J Polym Sci Polym Symp 1975;50:283.
[33] Kovacs AJ, Straupe C, Gonthier A. J Polym Sci, Polym Symp 1977;59:31.
[34] Kovacs AJ, Straupe C. Faraday Discuss Chem Soc 1979;68:225.
[35] Kovacs AJ, Straupe C. Cryst Growth 1980;48:210.
[36] Cheng SZH, Zhang AQ, Chen JH. J Polym Sci, Polym Phys Ed 1991;29:299.
[37] Cheng SZH, Zhang A, Barley JS, Chen J, Habenschuss A, Zschack PR. Macromolecules 1991;24:3937.
[38] Cheng SZD, Chen J, Barley JS, Zhang A, Habenschuss A, Zschack PR. Macromolecules 1992;25:1453.
[39] Vlèek P, Otoupalová J, Køí J, Composto RJ, Oslanec R. Polym Prepr 1997;38 (1):446.
[40] Trekoval J. Collect Czech Chem Commun 1973;38:3769.
[41] Trekoval J, Vlèek P. Chem Prum 1968;18:312.
[42] Amenitsch H, Bernstorff S, Kriechbaum M, Lombardo D, Mio H, Rappolt M, Laggner P. J Appl Crystallogr 1997;30:872.
[43] van Krevelen DW. Properties of polymers. Amsterdam: Elsevier, 1990.
[44] Song K, Krimm S. Macromolecules 1990;23:1946.